

Journal of Materials Chemistry A

Accepted Manuscript



This is an *Accepted Manuscript*, which has been through the Royal Society of Chemistry peer review process and has been accepted for publication.

Accepted Manuscripts are published online shortly after acceptance, before technical editing, formatting and proof reading. Using this free service, authors can make their results available to the community, in citable form, before we publish the edited article. We will replace this *Accepted Manuscript* with the edited and formatted *Advance Article* as soon as it is available.

You can find more information about *Accepted Manuscripts* in the [Information for Authors](#).

Please note that technical editing may introduce minor changes to the text and/or graphics, which may alter content. The journal's standard [Terms & Conditions](#) and the [Ethical guidelines](#) still apply. In no event shall the Royal Society of Chemistry be held responsible for any errors or omissions in this *Accepted Manuscript* or any consequences arising from the use of any information it contains.

Two Stable 3D Porous Metal-Organic Frameworks with High Performance for Gas Adsorption and Separation

Cite this: DOI: 10.1039/x0xx00000x

Received 00th January 2012,
Accepted 00th January 2012

DOI: 10.1039/x0xx00000x

www.rsc.org/

Shuo Yao, Dongmei Wang, Yu Cao, Guanghua Li, Qisheng Huo, and Yunling Liu*

Two porous MOFs, $[\text{NO}_3][\text{In}_3\text{O}(\text{C}_6\text{H}_4)_3] \cdot 4\text{DMF} \cdot 3\text{H}_2\text{O}$ (**JLU-Liu18**), $[\text{CdL}]\cdot 0.5\text{DMF}$ (**JLU-Liu19**) $\text{H}_2\text{L} = \text{pyridine-3,5-bis(phenyl-4-carboxylic acid)}$, have been solvothermally synthesized and structurally characterized. Both of the two compounds possess saturated coordination metal centre without open metal sites (OMSs) leading to the remarkable thermal and water vapour stability. **JLU-Liu18** displays a rare occurrence of 9-connected trinuclear $[\text{In}_3\text{O}(\text{CO}_2)_6\text{N}_3]$ secondary building units (SBUs) in a porous crystal with high adsorption for small molecule gases, especially for CO_2 (129 and $400 \text{ cm}^3 \text{ g}^{-1}$ at 273 K and 195 K under 1 bar). It also performs commendable selectivity for O_2 over N_2 and CO_2 , C_2H_6 , C_3H_8 over CH_4 . **JLU-Liu19** possesses outstanding performance for sieving small gases owing to its ultramicropores of 3.5 Å. Both of the two MOFs are promising materials for gas adsorption and purification.

Introduction

Environment and energy problems are hot issues concerned by the global world all this time. In recent years, the dramatic increasing level of atmospheric CO_2 resulting from anthropogenic emissions is one of the greatest environmental concerns facing our civilization.¹⁻³ Furthermore, regardless of the greenhouse effect, CO_2 is also an impurity in natural gas, biogas, post-combustion flue gases generated from coal-fired power stations and many other gas streams which will reduce energy conversion efficiency.⁴⁻⁶ Methane as the primary component of natural gas and biogas is considerable cleaner energy source for our daily life.⁷ However, a quantity of hydrocarbon impurities will reduce the utilization efficiency of methane. Therefore, exploring new materials that not only efficiently capture and sequester CO_2 but also purify methane from natural gas and biogas in order to improve the conversion rate is an issue that needed to be addressed as a matter of urgency.

Porous metal-organic frameworks (MOFs), which offer large surface areas, high void volumes, tunable pore size and chemical tenability, have been actively pursued in the past decades on account of their potential applications in gas storage and separation technologies towards small molecules.^{8,9} The promising performance is owing to the micropores within MOFs can be tuned by selecting kinds of ligands with different functional groups and diverse metal cores to construct a variety of metal-containing secondary building units (SBUs). The metal-containing SBUs can be mononuclear, bi-nuclear, tri-

nuclear, tetra-nuclear, hexa-nuclear, and even more.¹⁰ Particularly, the MOFs materials based on multi-nuclear SBUs exhibit high stability and permanent porosity after desolvation. Herein, we choose the heterofunctional ligand pyridine-3, 5-bis(phenyl-4-carboxylic acid) (H_2L) which containing carboxylate and pyridyl groups to construct new MOFs materials based on the following aspect: 1) the diverse coordinate mode of $-\text{COOH}$ and N donor with metal centre is facility to form the unique structure; 2) as a pyridyl derivative and attachable ligand instead of terminal coordinated molecule to increase connectivity of the net; 3) Up to now, only a few porous MOFs based on this ligand were reported.¹¹⁻¹⁶ Nevertheless, we successfully utilize this ligand and react with indium or cadmium metal source to generate two new MOFs materials, $[\text{NO}_3][\text{In}_3\text{O}(\text{C}_{19}\text{H}_{11}\text{NO}_4)_3] \cdot 4\text{DMF} \cdot 3\text{H}_2\text{O}$ (**JLU-Liu18**) and $[\text{Cd}(\text{C}_{19}\text{H}_{11}\text{NO}_4)] \cdot 0.5\text{DMF}$ (**JLU-Liu19**). In the two compounds, the terminal of metal ions is coordinated by pyridine groups leading to the metal centre saturated coordination without open metal sites (OMSs), which remarkably increasing the thermal and water vapour stability. To the best of our knowledge, most of the In-MOFs based on trinuclear $[\text{In}_3\text{O}(\text{O}_2\text{CR})_6]$ SBUs is usually 6-connected and possesses OMSs. However, **JLU-Liu18** is a rare occurrence of 9-connected $[\text{In}_3\text{O}(\text{CO}_2)_6\text{N}_3]$ SBUs. Compared with the nonporous MOF constructed by a shorter ligand,²⁵ **JLU-Liu19** with ultramicropores exhibits extraordinary and specific carbon capture and separation (CCS). It is worth noting that two compounds with air and water vapour stability exhibit high-

capacity adsorption and high-effect separation of small gases. The selectivity for CO₂/CH₄, C₂H₆/CH₄ and C₃H₈/CH₄ were appraised by the ideal adsorbed solution theory (IAST).

Experimental

Materials and Methods

All chemicals were obtained from commercial sources and used without further purification. Powder X-ray diffraction (PXRD) data were collected on a Rigaku D/max-2550 diffractometer with Cu K_α radiation ($\lambda = 1.5418 \text{ \AA}$). Elemental analyses (C, H, and N) were achieved by vario MICRO (Elementar, Germany). The thermal gravimetric analyses (TGA) were performed on TGA Q500 thermogravimetric analyzer used in air with a heating rate of 10 °C min⁻¹.

Synthesis of JLU-Liu18

Single crystals of compound **JLU-Liu18** were obtained by solvothermal reaction of In(NO₃)₃·4H₂O (12 mg, 0.03 mmol) and H₂L (5 mg, 0.015 mmol) in N,N-dimethylformamide (DMF) (2 mL)/1,4-dioxane (DOA) (0.6 mL) with HNO₃ (0.225 mL) (2.2 mL HNO₃ in 10 mL DMF) at 105 °C for 24 hours. The mixture was then cooled to room temperature. Colorless cubic crystals were obtained and air-dried (yield 40%, based on H₂L). Elemental analysis (%) Calcd for **JLU-Liu18** [NO₃][In₃O(C₁₉H₁₁NO₄)₃]·4DMF·3H₂O: C, 48.13; H, 3.72; N, 6.51, Found: C, 48.20; H, 3.98; N, 7.03. The experimental PXRD pattern is in good agreement with the simulated one based on the single-crystal X-ray data, indicating the purity of the as-synthesized product (Fig. S1†).

Synthesis of JLU-Liu19

Colorless block crystals of **JLU-Liu19** were obtained by solvothermal reaction of Cd(NO₃)₂·4H₂O (5 mg, 0.016 mmol) and H₂L (5 mg, 0.015 mmol) in DMF (1 mL) with HNO₃ (0.2 mL) (2.2 mL HNO₃ in 10 mL DMF) at 105 °C for 24 hours. The mixture was then cooled to room temperature. The crystals were collected and washed with DMF, then dried in air (yield 45% based on H₂L). Elemental analysis calcd (%) for **JLU-Liu19**, [Cd(C₁₉H₁₁NO₄)]·0.5DMF: C, 52.79; H, 3.11; N, 4.5; Found: C, 52.01; H, 3.05; N, 4.28. The experimental PXRD pattern agrees well with the simulated one based on the single-crystal X-ray data, indicating the purity of the as-synthesized product (Fig. S2†).

X-ray Crystallography

Crystallographic data for two compounds were collected on a Bruker Apex II CCD diffractometer using graphite-monochromated Mo-K_α ($\lambda = 0.71073 \text{ \AA}$) radiation at room temperature. The structures were solved by direct methods and refined by full-matrix least-squares on F^2 using version 5.1.¹⁷ All the metal atoms were located first, and then the oxygen and carbon atoms of the compound were subsequently found in difference Fourier maps. The hydrogen atoms of the ligand were placed geometrically. All non-hydrogen atoms were

refined anisotropically. The final formula was derived from crystallographic data combined with elemental and thermogravimetric analysis data. The detailed crystallographic data and selected bond lengths and angles for two compounds are listed in Table S1-3†, respectively. Crystallographic data for **JLU-Liu18** (1403645) and **JLU-Liu19** (1402651) have been deposited with Cambridge Crystallographic Data Centre. Data can be obtained free of charge upon request at www.ccdc.cam.ac.uk/data_request/cif. Topology information for the two compounds were calculated by TOPOS 4.0.¹⁸

Gas adsorption measurements

The N₂, H₂, O₂, Ar, CO₂, CH₄, C₂H₆ and C₃H₈ gas adsorption measurements were performed on a Micromeritics ASAP 2420 and a Micromeritics ASAP 2020 instrument. Before gas adsorption measurements, the samples were exchanged with fresh methanol 10 times for 2 days to completely remove the non-volatile solvent molecules, which can be proved by TGA analysis (Fig. S3-4†). The sample was activated by drying under a dynamic vacuum at room temperature for 1 hour. Before the measurement, the sample was dried again by using the 'outgas' function of the surface area analyzer for 10 h at 100 °C.

Results and discussion

Single-crystal X-ray diffraction analysis shows that **JLU-Liu18** crystallizes in the *R*-3*c* space group. As shown in Figure 1a, **JLU-Liu18** adopt the [In₃(μ₃-O)(CO₂)₆N₃] SBU with the bridging-O residing at the centre of the three indium atoms with In-O bonds of 2.0289(3)Å, while the three indium atoms are chelated by six carboxylate groups and three pyridyl groups. Although there are many similar SBUs composed of other metals have been reported in the literature,¹⁹⁻²⁴ the 9-connected [In₃(μ₃-O)(CO₂)₆N₃] trimer is really rare in reported InMOFs. From a topological point of view, the trinuclear indium cluster can be simplified to be a 9-connected node with tetrakaidecahedron geometry, and the ligand can be regarded as 3-connected node with triangular geometry. Consequently, the structure of **JLU-Liu18** can be described as a (3, 9)-connected network, which belongs to *xmz*²⁵ topology with a Schläfli symbol of (4².6)₃(4⁶.6²¹.8⁹). Furthermore, regarding the trinuclear indium cluster as a node and linked by the tridentate ligand, distorted cubic cages with a diameter of about 8.3 Å regardless of the Van der Waals radius can be clearly seen in the Figure 1c. As shown in Figure 1e, there are two types of tile of [4.6²] and [6⁶]. The PLATON calculation reveals a total solvent-accessible volume equal of 9488.4 Å³ per unit cell, which counts for approximately 62.0% of the cell volume, exhibiting high porosity and offering possibilities for gas adsorption.

The X-ray crystallographic analysis revealed that **JLU-Liu19** crystallizes in the *C*2/*c* space group. As depict in Figure 2a, each cadmium ion is five coordinated to four oxygen atoms and one nitrogen atom from five ligands and then forming

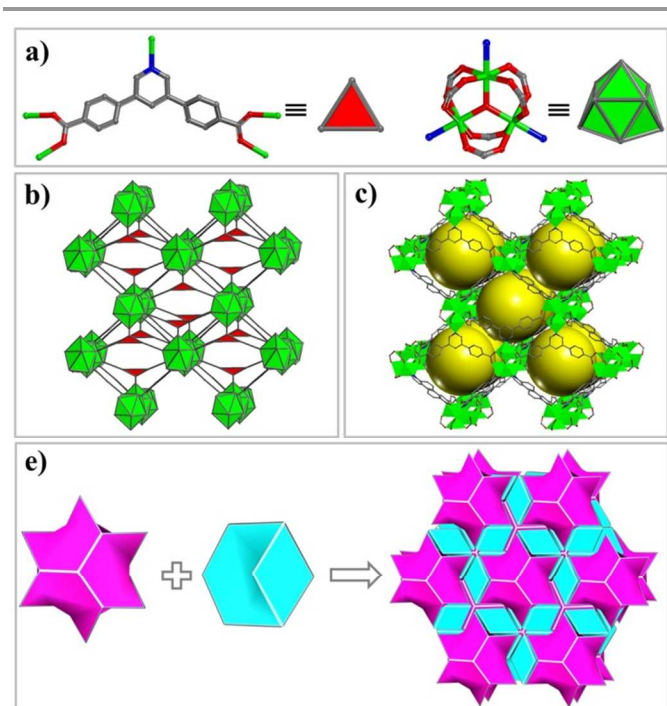


Fig. 1 Single-crystal structure for **JLU-Liu18**: (a) topology simplification of ligand and metal core. (b) polyhedron view of the *xnz* net. (c) pores in the framework shown as yellow spheres. (e) topological features of the compound displayed by tiling. Colour scheme: carbon = gray, nitrogen = blue, oxygen = red, indium = green. Guest molecules and H atoms have been omitted for clarity.

geometry of trigonal bipyramid. Similar, each independent ligand is coordinated to five cadmiums but presents the tetragonal pyramidal geometry structure. Therefore, the overall structure of **JLU-Liu19** possesses *bnn*²⁶ topology with a Schläfli symbol of $(4^6.6^4)$ (Fig. 2b). The topological feature displayed by tiling is shown in Figure 2c which possesses only one kind of tile of $[4^6.6^4]$. As shown in Figure 2d, all of the metal atoms in the structure are bridged by carboxyl groups to form an infinite rod-shaped metal-carboxylate building unit. The rod further connects with the others through ligands to form a layer and then extended by Cd-N bonding to generate a 3D framework. Furthermore, there exist 1D ultramicroporous channels with a diameter of ~ 3.5 Å along the z-axis regardless of the Van der Waals radius.

Thermal gravimetric analyses (TGA) under an atmospheric environment were then carried out to assess the thermal stability of the two compounds and the pore volume that occupy by guest molecules. The results show that **JLU-Liu18** framework can be stable up to about 350 °C with approximately 22% weight loss observed before 200 °C because of the removal of guest molecules (Fig. S3†). While **JLU-Liu19** is stable until 450 °C and it is approximately 10% weight loss observed before 200 °C for the removal of guest molecules (Fig. S4†). Both of the two compounds exhibit higher thermal stability than **JLU-Liu1** with octa-nuclear SBU.²⁷ It can be also observed that **JLU-Liu18** has more solvent occupied volume than **JLU-Liu19**, which indicates that **JLU-Liu18** is supposed to possess more open pore volume after desolvation. It should

be to note that both of the two compounds exhibit good air and water vapour stability. When exposed to air for several months or treated by water vapour for 1, 3, 6 and 12 hours, respectively, the frameworks of the two compounds still retain stability which can be proved by the crystallinity of PXRD (Fig. 3). The excellent stable behaviour of the two compounds is of extremely importance for their practical applications.

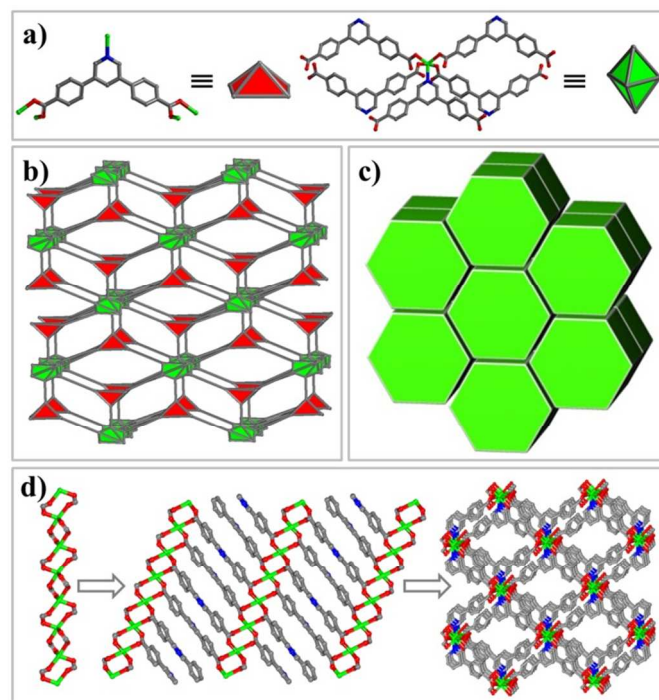


Fig. 2 Single-crystal structure for **JLU-Liu19**: (a) topology simplification of ligand and metal core. (b) polyhedron view of the *bnn* net. (c) topological features of the compound displayed by tiling. (d) the formation of 3D framework from 1D metal chain and 2D layer. Colour scheme: carbon = gray, nitrogen = blue, oxygen = red, cadmiums = green. Guest molecules and H atoms have been omitted for clarity.

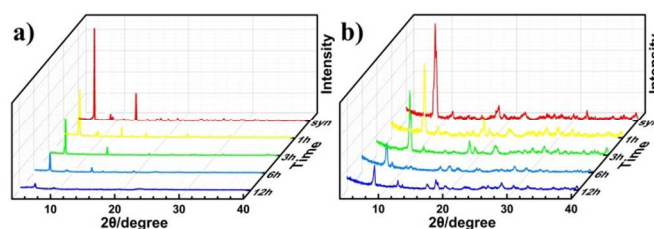


Fig. 3 PXRD patterns for **JLU-Liu18** (a) and **JLU-Liu19** (b) after exposed to water vapor for 1, 3, 6 and 12 hours, respectively.

The permanent porosity and surface areas of desolvated **JLU-Liu18** were probed by reversible N₂ sorption experiments at 77 K. The N₂ adsorption of activated **JLU-Liu18** reveals a reversible type-I isotherm characteristic of microporous material (Fig. 4). The BET surface areas and Langmuir surface areas for **JLU-Liu18** were calculated to be 1300 m² g⁻¹ and 1800 m² g⁻¹, respectively, which is about triple to the Mg analogues¹¹ and close to Ni and Fe analogues.¹² It is among the highest of all known InMOFs.^{28, 29} The micropore volume is 0.65 cm³ g⁻¹ which is close to the theoretical value of 0.72 cm³

g^{-1} . N_2 gas sorption isotherm of **JLU-Liu19** was also measured at 77 K under 1 bar, there is almost no N_2 adsorption (Fig. 4).

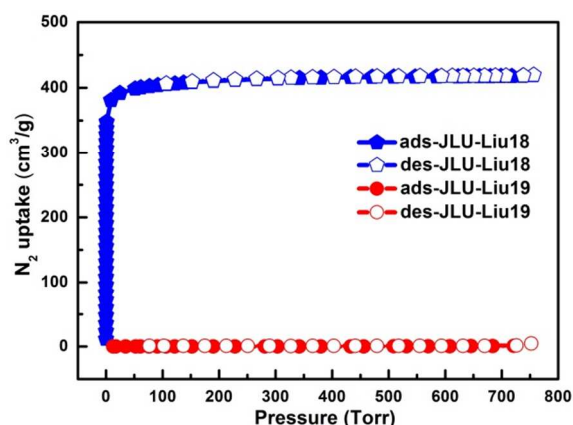


Fig. 4 N_2 sorption isotherms for **JLU-Liu18** (blue) and **JLU-Liu19** (red) at 77 K.

Both of the two MOFs explored the CO_2 adsorption performance. As shown in Figure 5a, the amount of CO_2 uptake for **JLU-Liu18** is 129 and $63 \text{ cm}^3 \text{ g}^{-1}$ at 273 and 298 K under 1 bar, respectively. Although large numbers of MOF with good CO_2 capture performance have been reported, it is still scarce for MOFs that forerach $100 \text{ cm}^3 \text{ g}^{-1}$ at 273 K and 1 bar. It is worthy mentioned that such high CO_2 uptake can be even compared to the MOFs with OMSs^{9, 30} or Lewis basic sites.³¹⁻³³ It is also ranks in the highest adsorption amount of CO_2 for In-MOFs (Table S4). Meanwhile, the CO_2 uptake at 195 K and 1 bar reaches $400 \text{ cm}^3 \text{ g}^{-1}$ (Fig. S5†), which is comparable to those of MOFs with mesopores.^{34, 35} To acquire further insight into CO_2 adsorption, the behaviour of the isosteric heat was calculated. The adsorption enthalpy of **JLU-Liu18** is 24.9 kJ mol^{-1} (Fig. 5b), indicating the strong interactions between the CO_2 molecules and host framework.

Although there is no N_2 adsorption for **JLU-Liu19**, the CO_2 adsorption was observed to be 56 and $42 \text{ cm}^3 \text{ g}^{-1}$ at 273 and 298 K under 1 bar (Fig. 5c). Albeit these values are lower than **JLU-Liu18**, it is considerable higher than many well-known MOFs without OMSs or uncoordinated N-donor sites.^{36, 37} It is also far beyond the Zn analogues.¹⁴⁻¹⁶ **JLU-Liu19** shows a near-zero coverage Q_{st} value of 34.2 kJ mol^{-1} (Fig. 5d) which surpass **JLU-Liu18** and compare to MOFs materials with OMSs,^{38, 39} indicating the strong host-guest C-H...O interaction between the CO_2 molecules and phenyl rings in the host framework, and the quadrupole-quadrupole interactions between the CO_2 molecules.⁴⁰ Considerable uptake of CO_2 with N_2 not adsorbed is known for ultramicroporous MOFs. It is commendable for ultramicroporous MOFs with considerable uptake of CO_2 but no N_2 adsorption. **JLU-Liu19** fortunately possess the uncommon performance, which can be ascribed to the small internal channel size of 3.5 \AA lying intermediate among that of N_2 (3.64 \AA), CH_4 (3.87 \AA) and CO_2 (3.3 \AA). The unusual cavity diameter can be regarded as ultramicroporous,^{13, 41, 42} which leading to excellent sieving and selective adsorption performance.

On account of the high BET and adsorption performance of CO_2 for **JLU-Liu18**, we investigate its adsorption performance for some other small gases. As shown in Figure S6†, the low-pressure uptake for H_2 is completely reversible and the adsorption amount is 1.81 wt% ($203 \text{ cm}^3 \text{ g}^{-1}$) and 1.34 wt% ($150 \text{ cm}^3 \text{ g}^{-1}$) at 77 and 87 K under 1 bar, which are quite comparable with the highly porous MOFs under the same conditions.^{43, 44} Furthermore, the maximum adsorption amount of O_2 is $529 \text{ cm}^3 \text{ g}^{-1}$ at 77 K (Fig. S7†), which is comparable to those of highly porous MOFs.^{45, 46} Comparing with N_2 gas sorption isotherms measured at the same condition, O_2 is more favourably adsorbed over N_2 with a O_2/N_2 selectivity of 1.24 at 0.2 P/P₀, such sorption behaviour is commensurate with Fe/Cu-BTC and Co/Cu-BTC with OMSs.⁴⁷ However, as far as saturated coordination MOFs to be concerned, the O_2/N_2 selectivity of **JLU-Liu18** is relatively high. With the temperature increasing, O_2 loadings decrease to be 9 and $5 \text{ cm}^3 \text{ g}^{-1}$ (Fig. S8†). The Q_{st} at the highest loadings is observed to be 16 kJ mol^{-1} (Fig. S9†), which exceed the highest Q_{st} in metal-substituted Cu-BTC,⁴⁷ deducing the stronger interactions between O_2 and host framework.

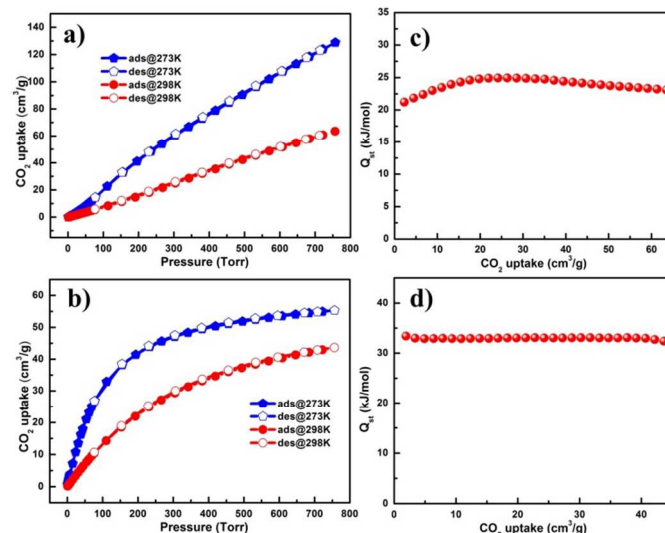


Fig. 5 CO_2 adsorption isotherms for **JLU-Liu18** (a) and **JLU-Liu19** (b) at 273 and 298 K under 1 bar, respectively. Q_{st} of CO_2 for **JLU-Liu18** (c) and **JLU-Liu19** (d).

With stable and permanent porosity, **JLU-Liu18** is evaluated its potential storage and selective separation application for CO_2 and small hydrocarbons, which are the prim composition of flue gas, natural gas and biogas. The adsorption isotherms for CH_4 , C_2H_6 and C_3H_8 are measured at 273 and 298 K under 1 bar, respectively. The maximum adsorption for CH_4 is 23 and $12 \text{ cm}^3 \text{ g}^{-1}$, C_2H_6 is 128 and $92 \text{ cm}^3 \text{ g}^{-1}$ and C_3H_8 is 138 and $116 \text{ cm}^3 \text{ g}^{-1}$, respectively (Fig. S10 to S12†).⁴⁸ At zero loading, Q_{st} of CH_4 , C_2H_6 and C_3H_8 adsorption is 18, 25 and 44 kJ mol^{-1} , respectively, as estimated from the sorption isotherms at 273 and 298 K (Fig. S13 to S15†). It indicated that the unique cage structures of **JLU-Liu18** with medium pore size induce stronger interaction with larger hydrocarbons than the smaller ones.⁴⁹ The types of interaction are presumably the combined

effects of the van der Waals host-guest interactions and the electrostatic host-guest interactions in the system.⁵⁰

In order to estimate the practical separate ability for CO₂, theoretical gas mixtures of CO₂/CH₄ (5 % and 95%, 50% and 50%) are conducted by the IAST model which is a common method to predict binary mixture adsorption from experimental single-component isotherms. We successfully use the dual-site Langmuir-Freundlich equation to fit the data.⁵¹⁻⁵³ As shown in Figure 6a, the model fits the isotherms at 298 K very well ($R^2 > 0.9999$). The fitting parameters were then used to predict multi-component adsorption with IAST (listed in Table S5†). At 298 K and 1 bar, the selectivity of CO₂ over CH₄ for **JLU-Liu18** according to the experimental data is 5.4 and 4.5 (Fig. 5b), which surpass the values of MIL-53(Al), MOF-5 and some carbon materials under the same measurement conditions.⁵⁴⁻⁵⁶ The potential application for the industrially important small hydrocarbon separation is also explored for **JLU-Liu18** by IAST. As shown in Figure 5d, the obtained values of the resulting selectivity of C₂H₆ over CH₄, C₃H₈ over CH₄ for equimolar is 13.1, 108.2 at 298 K and 1 bar, respectively. It is noteworthy that the selectivity of C₃H₈ over CH₄ is much higher than the very high value for UTSA-35a⁵⁷ and JLU-Liu5.⁵⁸

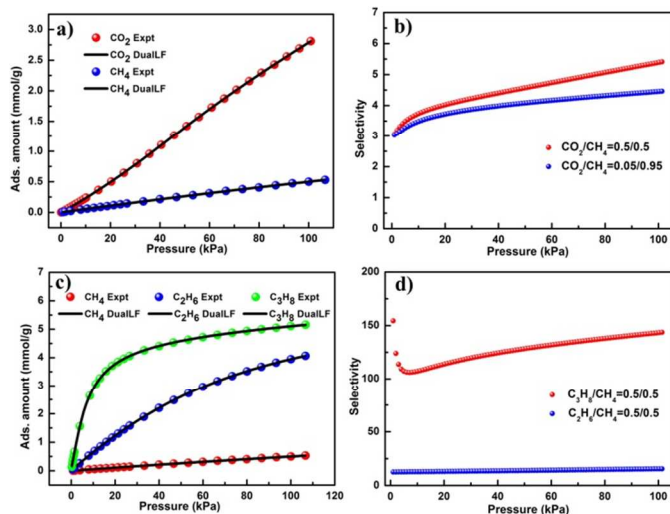


Fig. 6 CO₂, CH₄, C₂H₆ and C₃H₈ adsorption isotherms at 298 K along with the dual-site Langmuir Freundlich (DSLFF) fits (a, c); Gas mixture adsorption selectivity are predicted by IAST at 298 K and 100 kPa for **JLU-Liu18** (b, d).

Conclusions

In summary, we have successfully synthesized two novel microporous MOFs based on a tridentate heterofunctional ligand with indium nitrate and cadmium nitrate. Both of the two compounds exhibit high thermal and water vapour stability as well as highlighted adsorption performance for small gases. Meanwhile, **JLU-Liu18** also displays outstanding selectivity for O₂/N₂, CO₂/CH₄, C₂H₆/CH₄ and C₃H₈/CH₄. **JLU-Liu19** with unique ultramicropores possesses uncommon sieving effect for the gases with different kinetic diameter. It is promising to apply these emerging porous materials to the field

of industrially important gas storage and separation of in the near future.

Acknowledgements

This work was supported by the National Natural Science Foundation of China (Nos. 21373095, 21371067 and 21171064).

Notes and references

State Key Laboratory of Inorganic Synthesis and Preparative Chemistry, College of Chemistry, Jilin University, Changchun 130012, P. R. China. Fax: +86-431-85168624; Tel: +86-431-85168614; E-mail: yunling@jlu.edu.cn

† Electronic Supplementary Information (ESI) available: [materials and methods, crystal data and structure refinement, structure information, XRD, TGA, gases adsorption and adsorptive selectivity. CCDC 1403645, 1402651]. See DOI: 10.1039/b000000x/

- Z. Zhang, Z. Z. Yao, S. Xiang and B. Chen, *Energy Environ. Sci.*, 2014, **7**, 2868-2899.
- E. D. Bloch, L. J. Murray, W. L. Queen, S. Chavan, S. N. Maximoff, J. P. Bigi, R. Krishna, V. K. Peterson, F. Grandjean, G. J. Long, B. Smit, S. Bordiga, C. M. Brown and J. R. Long, *J. Am. Chem. Soc.*, 2011, **133**, 14814-14822.
- N. MacDowell, N. Florin, A. Buchard, J. Hallett, A. Galindo, G. Jackson, C. S. Adjiman, C. K. Williams, N. Shah and P. Fennell, *Energy Environ. Sci.*, 2010, **3**, 1645-1669.
- S. Chaemchuen, N. A. Kabir, K. Zhou and F. Verpoort, *Chem. Soc. Rev.*, 2013, **42**, 9304-9332.
- J. R. Li, J. Sculley and H. C. Zhou, *Chem. Rev.*, 2012, **112**, 869-932.
- D. M. D'Alessandro, B. Smit and J. R. Long, *Angew. Chem., Int. Ed.*, 2010, **49**, 6058-6082.
- Y. He, W. Zhou, G. Qian and B. Chen, *Chem. Soc. Rev.*, 2014, **43**, 5657-5678.
- K. Sumida, D. L. Rogow, J. A. Mason, T. M. McDonald, E. D. Bloch, Z. R. Herm, T.-H. Bae and J. R. Long, *Chem. Rev.*, 2012, **112**, 724-781.
- P. Nugent, Y. Belmabkhout, S. D. Burd, A. J. Cairns, R. Luebke, K. Forrest, T. Pham, S. Ma, B. Space, L. Wojtas, M. Eddaoudi and M. J. Zaworotko, *Nature*, 2013, **495**, 80-84.
- D. J. Tranchemontagne, J. L. Mendoza-Cortes, M. O'Keeffe and O. M. Yaghi, *Chem. Soc. Rev.*, 2009, **38**, 1257-1283.
- Q. Zhai, Q. Lin, T. Wu, S. T. Zheng, X. Bu and P. Feng, *Dalton Trans.*, 2012, **41**, 2866.
- J. Jia, X. Lin, C. Wilson, A. J. Blake, N. R. Champness, P. Hubberstey, G. Walker, E. J. Cussen and M. Schroder, *Chem. Commun.*, 2007, 840-842.
- Y. S. Wei, K. J. Chen, P. Q. Liao, B. Y. Zhu, R. B. Lin, H. L. Zhou, B. Y. Wang, W. Xue, J. P. Zhang and X. M. Chen, *Chem. Sci.*, 2013, **4**, 1539.
- T. Ding, L. D. Ren, X. D. Du, L. Quan, Z. W. Gao, W. Q. Zhang and C.-Z. Zheng, *CrystEngComm*, 2014, **16**, 7790.
- R. Yun, Y. Jiang, S. Luo and C. Chen, *RSC Adv.*, 2014, **4**, 36845-36848.
- P.-P. Cui, X. D. Zhang, Y. Zhao, K. Chen, P. Wang and W. Y. Sun, *Microporous Mesoporous Mater.* 2015, **208**, 188-195.

17. Sheldrick, G. M. SHELXTL-NT, version 5.1; Bruker AXS Inc., Madison, WI, 1997.
18. V. A. Blatov, A. P. Shevchenko, D. M. Proserpio, *Cryst. Growth Des.*, 2014, **14**, 3576-3683.
19. J. Jia, X. Lin, C. Wilson, A. J. Blake, N. R. Champness, P. Hubberstey, G. Walker, E. J. Cussen and M. Schroder, *Chem. Commun.*, 2007, 840-842.
20. Q. Zhai, Q. Lin, T. Wu, S. T. Zheng, X. Bu and P. Feng, *Dalton Trans.*, 2012, **41**, 2866-2868.
21. W. Bury, E. Chwojnowska, I. Justyniak, J. Lewiński, A. Affek, E. Zygadło-Monikowska, J. Bąk and Z. Florjańczyk, *Inorg. Chem.*, 2012, **51**, 737-745.
22. S. T. Zheng, T. Wu, C. Chou, A. Fuhr, P. Feng and X. Bu, *J. Am. Chem. Soc.*, 2012, **134**, 4517-4520.
23. R. Eguchi, S. Uchida and N. Mizuno, *Angew. Chem., Int. Ed.*, 2012, **51**, 1635-1639.
24. X. Zhao, X. Bu, Q. G. Zhai, H. Tran and P. Feng, *J. Am. Chem. Soc.*, 2015, **137**, 1396-1399.
25. X. M. Zhang, Y. Z. Zheng, C. R. Li, W. X. Zhang and X. M. Chen, *Cryst. Growth Des.*, 2007, **7**, 980-983.
26. N. L. Rosi, J. Kim, M. Eddaoudi, B. Chen, M. O'Keeffe and O. M. Yaghi, *J. Am. Chem. Soc.*, 2005, **127**, 1504-1518.
27. J. Luo, J. Wang, G. Li, Q. Huo and Y. Liu, *Chem. Commun.*, 2013, **49**, 11433-11435.
28. X. Gu, Z. H. Lu and Q. Xu, *Chem. Commun.*, 2010, **46**, 7400-7402.
29. M. Du, M. Chen, X. G. Yang, J. Wen, X. Wang, S. M. Fang and C.-S. Liu, *J. Mater. Chem. A*, 2014, **2**, 9828-9834.
30. D. D. Zhou, C. T. He, P. Q. Liao, W. Xue, W. X. Zhang, H. L. Zhou, J. P. Zhang and X. M. Chen, *Chem. Commun.*, 2013, **49**, 11728-11730.
31. A. Demessence, D. M. D'Alessandro, M. L. Foo and J. R. Long, *J. Am. Chem. Soc.*, 2009, **131**, 8784-8786.
32. R. Vaidhyanathan, S. S. Iremonger, G. K. H. Shimizu, P. G. Boyd, S. Alavi and T. K. Woo, *Science*, 2010, **330**, 650-653.
33. N. Planas, A. L. Dzubak, R. Poloni, L. C. Lin, A. McManus, T. M. McDonald, J. B. Neaton, J. R. Long, B. Smit and L. Gagliardi, *J. Am. Chem. Soc.*, 2013, **135**, 7402-7405.
34. X. Gu, Z. H. Lu and Q. Xu, *Chem. Commun.*, 2010, **46**, 7400-7402.
35. S. Ma and H. C. Zhou, *Chem. Commun.*, 2010, **46**, 44-53.
36. X. Zheng, L. Zhou, Y. Huang, C. Wang, J. Duan, L. Wen, Z. Tian and D. Li, *J. Mater. Chem. A*, 2014, **2**, 12413-12422.
37. L. Hou, L. N. Jia, W. J. Shi, Y. Y. Wang, B. Liu and Q. Z. Shi, *Dalton Trans.*, 2013, **42**, 3653-3659.
38. S. Couck, J. F. M. Denayer, G. V. Baron, T. Rémy, J. Gascon and F. Kapteijn, *J. Am. Chem. Soc.*, 2009, **131**, 6326-6327.
39. A. N. Dickey, A. Ö. Yazaydin, R. R. Willis and R. Q. Snurr, *Can. J. Chem. Eng.*, 2012, **90**, 825-832.
40. M. Du, C. P. Li, M. Chen, Z. W. Ge, X. Wang, L. Wang and C. S. Liu, *J. Am. Chem. Soc.*, 2014, **136**, 10906-10909.
41. L. J. McCormick, S. G. Duyker, A. W. Thornton, C. S. Hawes, M. R. Hill, V. K. Peterson, S. R. Batten and D. R. Turner, *Chem. Mater.*, 2014, **26**, 4640-4646.
42. K. A. Forrest, T. Pham, A. Hogan, K. McLaughlin, B. Tudor, P. Nugent, S. D. Burd, A. Mullen, C. R. Cioce, L. Wojtas, M. J. Zaworotko and B. Space, *J. Phys. Chem. C*, 2013, **117**, 17687-17698.
43. S. J. Bao, R. Krishna, Y. B. He, J. S. Qin, Z. M. Su, S. L. Li, W. Xie, D. Y. Du, W. W. He, S. R. Zhang and Y. Q. Lan, *J. Mater. Chem. A*, 2015, **3**, 7361-7367.
44. S. T. Zheng, T. Wu, C. Chou, A. Fuhr, P. Feng and X. Bu, *J. Am. Chem. Soc.*, 2012, **134**, 4517-4520.
45. Y. E. Cheon, J. Park and M. P. Suh, *Chem. Commun.*, 2009, 5436-5438.
46. S. Ma, X. S. Wang, D. Yuan and H. C. Zhou, *Angew. Chem., Int. Ed.*, 2008, **47**, 4130-4133.
47. D. F. Sava Gallis, M. V. Parkes, J. A. Greathouse, X. Zhang and T. M. Nenoff, *Chem. Mater.*, 2015, **27**, 2018-2025.
48. H. Xu, J. Cai, S. Xiang, Z. Zhang, C. Wu, X. Rao, Y. Cui, Y. Yang, R. Krishna, B. Chen and G. Qian, *J. Mater. Chem. A*, 2013, **1**, 9916.
49. F. Wang, H.-R. Fu, D.-C. Hou and J. Zhang, *Cryst. Growth Des.*, 2014, **14**, 6467-6471.
50. K. Liu, B. Li, Y. Li, X. Li, F. Yang, G. Zeng, Y. Peng, Z. Zhang, G. Li, Z. Shi, S. Feng and D. Song, *Chem. Commun.*, 2014, **50**, 5031-5033.
51. W. Lu, D. Yuan, J. Sculley, D. Zhao, R. Krishna and H. C. Zhou, *J. Am. Chem. Soc.*, 2011, **133**, 18126-18129.
52. S. D. Burd, S. Ma, J. A. Perman, B. J. Sikora, R. Q. Snurr, P. K. Thallapally, J. Tian, L. Wojtas and M. J. Zaworotko, *J. Am. Chem. Soc.*, 2012, **134**, 3663-3666.
53. H. Zhao, Z. Jin, H. Su, J. Zhang, X. Yao, H. Zhao and G. Zhu, *Chem. Commun.*, 2013, **49**, 2780-2782.
54. H. Wang, X. Zeng and D. Cao, *J. Mater. Chem. A*, 2014, **2**, 11341.
55. Z. Xiang, X. Peng, X. Cheng, X. Li and D. Cao, *J. Phys. Chem. C*, 2011, **115**, 19864-19871.
56. Z. Zhang, S. Xiang, K. Hong, M. C. Das, H. D. Arman, M. Garcia, J. U. Mondal, K. M. Thomas and B. Chen, *Inorg. Chem.*, 2012, **51**, 4947-4953.
57. Y. He, Z. Zhang, S. Xiang, F. R. Fronczek, R. Krishna and B. Chen, *Chem. Commun.*, 2012, **48**, 6493-6495.
58. D. Wang, T. Zhao, Y. Cao, S. Yao, G. Li, Q. Huo and Y. Liu, *Chem. Commun.*, 2014, **50**, 8648-8650.